Elliptically Polarized High-Order Harmonic Emission from Molecules in Linearly Polarized Laser Fields

Xibin Zhou,* Robynne Lock, Nick Wagner, Wen Li, Henry C. Kapteyn, and Margaret M. Murnane
JILA and Department of Physics, University of Colorado, Boulder, Colorado 80309, USA
(Received 29 August 2008; published 20 February 2009)

We perform an accurate polarimetry measurement of high-order harmonic emission from aligned molecules. We find that harmonic emission from N_2 can be strongly elliptically polarized even when driven by linearly polarized laser fields. These data have broad implications for understanding molecules in strong fields because they cannot be explained by simple theories based on the strong field approximation and single active electron models. Finally, this work also shows that it is possible to engineer the polarization properties of harmonic emission by carefully preparing a molecular medium.

DOI: 10.1103/PhysRevLett.102.073902 PACS numbers: 42.65.Ky, 42.65.Re

High-order harmonic generation (HHG) results from the extreme distortion of an electron wave function of an atom or molecule in the presence of a strong femtosecond laser field. Using a simple analogy, an atom or molecule driven by a strong laser field behaves like an antenna—the radiated field will depend on the shape of the antenna, which in the case of HHG is the shape and orientation of the molecular orbital [1–7]. In a quantum picture, the HHG power spectrum is the Fourier transform of the dipole acceleration [8]. Thus, to accurately describe HHG, a full time-dependent multielectron wave function (including outer valence electrons) is required, which is challenging due to the required computation power.

Fortunately, a simple semiclassical three step model can be used to understand much of the physics of the HHG process [9,10]. In the 3-step model, the harmonic power spectrum generated from aligned molecules can be expressed as $S(\omega, \theta) = N^2(\theta)\omega^4 |a[k(\omega)]\boldsymbol{d}(\omega, \theta)|^2$ [1], where θ is the angle between the driving laser polarization and the molecular axis, $N(\theta)$ is proportional to the angle-dependent ionization rate, $a[k(\omega)]$ is the complex amplitude of the return electron wave packet, and $\boldsymbol{d}(\omega, \theta) = \langle \psi_c = e^{iky}|\mathbf{r}|\psi_g(\mathbf{r}, \theta)\rangle$ is the dipole matrix element between the recombining plane wave and the ground state highest occupied molecular orbital (HOMO). However, two important approximations are usually made in the 3-step model. First, due to the sequential nature of tunnel ionization, a single active electron approximation (SAEA) is used. Multielectron effects such as the indistinguishability of electrons and spin statistics are neglected [11]. In addition, a single ionization channel is assumed, where only the ground state of the cation is accessed. Second and more importantly, in the strong field approximation (SFA), the influence of the Coulomb potential on the recolliding electron is not considered [12]—in most cases, an electronic plane wave was used. The limitations of these approximations are not clear, particularly for molecules with closely lying cation states or undergoing structural changes [13]. Such questions have motivated intense theoretical efforts to extend the 3-step model beyond the SFA and SAEA [11,12,14]. However, the validity of these new and more sophisticated theories needs to be tested carefully with experiments.

In principle, the amplitude, phase, and polarization of the HHG emission can be measured and used to extract the electronic structure of molecules from the transition dipole matrix element. However, until very recently, only the intensity of high harmonic emission was measured. Fortunately, new approaches have allowed the phase of HHG to be determined [7,15]. In this Letter, we perform a full and accurate polarization measurement of high harmonic emission from aligned molecules for the first time. Surprisingly, we find that harmonic emission from N_2 can be strongly elliptically polarized even when driven by linearly polarized laser fields. Our findings differ from previously published results [16], where only linearly polarized harmonic emission was observed, because we achieve stronger molecular alignment and better signal-to-noise ratio ($1 \sim 2\%$ uncertainty), allowing us to detect an elliptically polarized HHG emission when molecules are driven by linearly polarized laser fields. These findings cannot be explained by a plane wave SFA and will be very useful to benchmark new and more complete theories of molecules in strong fields. Moreover, our results present a straightforward and efficient way to generate circularly polarized harmonic beams for applications in molecular and materials science.

The polarization state of harmonic emission from molecules is especially interesting for the following reasons. As shown in Fig. 1(a), in general, the complex amplitude of the harmonic field from a molecule has two components, parallel ($\boldsymbol{y}$) and perpendicular ($\boldsymbol{x}$) to the laser polarization, respectively. (Any component along the laser propagation direction cannot be phase matched.) $E_y(\omega, \theta) = |E_y(\omega, \theta)| \exp[i\Phi_y(\omega, \theta)]$ and $E_x(\omega, \theta) = |E_x(\omega, \theta)| \times \exp[i\Phi_x(\omega, \theta)]$ depend both on the harmonic frequency ω and angle θ. In theory, both HHG components should yield the same reconstruction of a molecular orbital [17].

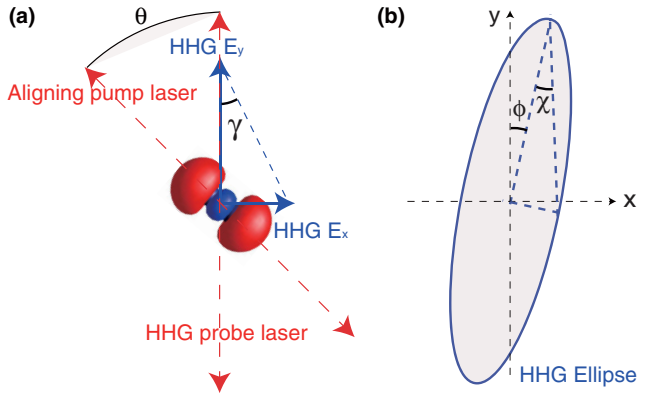

FIG. 1 (color online). High harmonic generation from aligned N_2. (a) HHG components parallel and perpendicular to the probe laser polarization can be generated. The angle γ is defined by $\tan(\gamma) = |E_x|/|E_y|$, where $\boldsymbol{x}$ and $\boldsymbol{y}$ are the lab frame axes. (b) The orientation angle ϕ of the HHG ellipse is defined as the angle between the major axis of the ellipse (max. transmission direction through polarizer) and the $\boldsymbol{y}$ axis. The angle χ is defined by $\tan(\chi) = \varepsilon$, where ε is the ellipticity. ϕ and θ are positive for clockwise rotation from the $\boldsymbol{y}$ direction and negative for counterclockwise rotation.

Moreover, according to the 3-step model, the ratio between the $\boldsymbol{x}$ and $\boldsymbol{y}$ components can be written as $|E_x(\omega, \theta)/E_y(\omega, \theta)|^2 = |d_x(\omega, \theta)/d_y(\omega, \theta)|^2$, which is independent of the angle-dependent ionization and is directly related to the transition dipole in these two directions. Finally, from the polarization properties of the HHG emission [the orientation angle ϕ and the ellipticity ε as defined in Fig. 1(b)], we can map out the phase difference $\delta = \Phi_x - \Phi_y$ between the $\boldsymbol{x}$ and $\boldsymbol{y}$ components. Again, because the ionization and acceleration steps are common for the two components, this phase difference is not entangled with the intrinsic phase accumulated while the electron oscillates in the continuum. Thus, measuring the polarization properties of HHG should allow us to study the ionization and recombination processes in HHG separately and also enable critical comparison with theory.

In our experiments, linearly polarized pump and probe pulses from a Ti: Sapphire amplifier system are focused (noncollinearly) into a molecular gas. The 120 fs pump pulse is focused by a 75 cm lens to an intensity of $4 \sim 5 \times 10^{13}$ W/cm^2, and is used to create a rotational wave packet in the molecular sample. The 30 fs probe pulse is focused using a 40 cm lens to an intensity of 2×10^{14} W/cm^2 and generates harmonics from the aligned molecules. Both foci are positioned $\approx$150 μm from a supersonic gas jet, with a 150 μm orifice diameter and 700 $\sim$ 800 Torr backing pressure. The rotational temperature of the gas was estimated to be 100 K and $\langle\cos^2\theta\rangle$ is estimated to be 0.65 when the molecules are aligned. This high degree of alignment improves the measurement precision compared with past experiments, allowing us to observe a strong HHG component perpendicular to the laser polarization. A computer controlled half-wave plate in the alignment beam controls the relative angle θ between the polarization of the pump and probe, while a second half-wave plate in the common path of the pump and probe beams can rotate the polarization of both beams together.

To measure the polarization of the harmonic emission, the HHG beam was reflected from two gold mirrors (consisting of a gold layer of 250 nm coated on a superpolished substrate) at an incident angle of 45°. These mirrors act as an EUV polarizer, selectively reflecting s polarization. The HHG beam was spectrally analyzed using an EUV spectrometer (containing a grazing-incidence cylindrical gold mirror and EUV grating) and finally detected using an EUV CCD camera (Andor). The transmission of the EUV spectrometer weakly depends on the incident light polarization. Because of the decreasing reflection efficiency of the gold mirrors at shorter wavelengths, only harmonics below the 31st are observed. The intensity extinction ratio $\boldsymbol{e}$ [defined as $R_p(\omega)/R_s(\omega)$, where R_p and R_s are the intensity reflectance of the detection system for p- and s-polarized HHG light, respectively) is carefully measured using HHG generated from isotropic molecules and atoms: $\boldsymbol{e}$ monotonically decreases from 0.08 at harmonic order 13, to 0.005 at harmonic 31. Note that the HHG beam can be partially polarized due to spatial and temporal variations in the HHG field [18]. Thus, the extinction ratio measured could be contaminated by any unpolarized HHG emission. However, the measured extinction ratio $\boldsymbol{e}$ is consistent with the calculated value for the gold mirrors based on optical constants, within an error of 0.015 for all harmonic orders observed [19]. Thus, we conclude that the harmonic emission is effectively fully polarized and that the HHG ellipse parameters (ϕ and ε) are constant temporally and spatially [18].

If the polarizations of the pump and probe beams are parallel, the molecular angular distribution is cylindrically symmetric around the laser polarization. Thus, harmonic emission is always polarized along the laser polarization direction. To investigate the polarization of the harmonics as a function of molecular orientation, we varied the angle between the aligning pump laser and the HHG-generating probe pulse (see Fig. 1), while fixing the time delay at a full revival for N_2 and a 3/4 revival for CO_2, where the molecules are strongly aligned. When the cylindrical symmetry around the probe laser polarization is broken, a component of harmonic emission perpendicular to the driving laser polarization should be observable experimentally.

We first analyze the intensity ratio between the parallel and perpendicular components of harmonic emission as a function of angle θ. The ratio between the measured HHG intensity when the harmonic generating laser is parallel and perpendicular to the transmission axis (s polarization) of the EUV polarizer is equal to $[\boldsymbol{e}I_y(\theta) + I_x(\theta)]/[\boldsymbol{e}I_x(\theta) + I_y(\theta)]$, where $I_x(\theta) = |E_x(\theta)|^2$ and $I_y(\theta) = |E_y(\theta)|^2$. Since

$eI_x(\theta) \ll I_y(\theta)$, subtracting the measured e from this ratio gives the true intensity ratio between the y and x components. The intensity ratios for N_2 and CO_2 molecules are plotted in Figs. 2(a) and 2(b) for different harmonic orders and relative angles. We obtain a ratio of zero at $\theta = -90°$, 0°, and 90°, which confirms the accuracy of our background subtraction procedure. Comparing the intensity ratios of the HHG polarization components for N_2 and CO_2 shown in Fig. 2, we can clearly see differences. For N_2, the intensity ratio increases between harmonics 17 and 23, and does not change very much for harmonics above 23. For CO_2, however, the ratio decreases between harmonic orders 15 and 21, but then increases quickly for harmonic orders above 23. This is because the y component from aligned CO_2 reaches a minimum due to two-center interference effects between harmonic orders 23 and 27 [7]. The HHG intensities of both the x and y components in this region are much smaller for CO_2 than for N_2, which leads to lower data quality—such as negative values and asymmetry with respect to 0°.

The polarization properties of the harmonic emission not only depend on the amplitudes of the x and y components, but also on their phase difference δ. If δ is 0 or π, the HHG emission will still be linearly polarized, but the nonzero perpendicular component E_x will rotate the HHG polarization away from the driving laser polarization direction by an angle given by γ. For other values of δ between 0 and π, the HHG will be elliptically polarized, and the orientation angle ϕ will be less than γ. Particularly, for $\delta = \pi/2$, the major axis of the HHG ellipse will be in the direction of the driving laser polarization. To implement a full polarization characterization, we rotate the relative angle θ between the pump and probe from −90° to 90°, in 10° steps. For each pump-probe angle, we rotate the second wave plate (which rotates the pump and probe polarizations together) by 360°, in 4° steps. We then fit the polarimetry scan data using the formula $I(\alpha) = a\cos[2(\alpha - \phi)] + c$, where α is the angle between the polarizer transmission axis and probe laser polarization. For each polarimetry scan, the positions of the maximum and minimum intensity [$I_{\min}(\theta)$ and $I_{\max}(\theta)$] correspond to the orientation angles of the major and minor axes of the HHG ellipse.

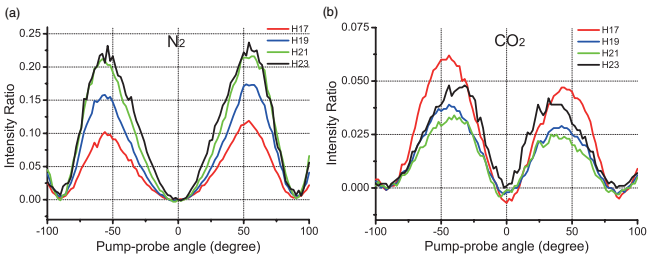

FIG. 2 (color online). Ratio between the perpendicular (x) and parallel (y) components of the HHG field $I_x(\theta)/I_y(\theta)$: (a) for N_2 and (b) for CO_2 molecules.

The extracted orientation angle ϕ of the HHG ellipse for N_2 is plotted in Fig. 3(a). For harmonic orders below 19, the major axis of the HHG ellipse rotates in the same direction as the molecular axis, while for orders greater than 19, the major axis rotates in the opposite direction. The change of orientation angle of the HHG ellipse reaches 20°, indicating that a stronger molecular alignment was achieved in our sample than was achieved in previous work [16], where the change in orientation angle was less than 10°.

For elliptically polarized light, the ratio between the minimum and maximum transmitted intensity of the polarimetry scan $I_{\min}(\theta)/I_{\max}(\theta)$ is given by $[I_{\text{minor}}(\theta) + eI_{\text{major}}(\theta)]/[I_{\text{major}}(\theta) + eI_{\text{minor}}(\theta)] \approx I_{\text{minor}}(\theta)/I_{\text{major}}(\theta) + e$, where I_{minor} and I_{major} are the intensity of the minor and major axis of the HHG ellipse. Therefore, the ellipticity of the harmonic emission, defined as $\varepsilon(\omega, \theta) = \sqrt{I_{\text{minor}}(\omega, \theta)/I_{\text{major}}(\omega, \theta)}$, can be extracted from the polarimetry measurement. Figure 4(a) plots the extracted ellipticity ε for different harmonic orders at orientation angles $\theta = 40°$, 50°, and 60° for N_2. These data show that harmonics from aligned N_2 molecules can be strongly elliptically polarized, with ellipticity up to 0.35 for harmonic orders near 21. In contrast, for CO_2 the measured ellipticity is relatively small (<0.1), only slightly above the noise. Thus, the perpendicular HHG components of CO_2 rotate the predominantly linearly polarized HHG without introducing significant ellipticity. As shown in Fig. 3(b), this rotation of the polarization is in the opposite direction to the rotation of the molecular axis.

We note that the HHG yield is very sensitive to any ellipticity in the driving laser beam that can be induced by various optics in the path (e.g., imperfect half-wave plate or vacuum window) [18]. Experimentally, we minimized the residual ellipticity by using broad bandwidth wave plates and thin (1 mm), low-stress, glass windows. We also average two 180° sections of the acquired 360° polarimetry scan, which strongly reduces the effect of residual ellipticity from the imperfect wave plate. Since any resid-

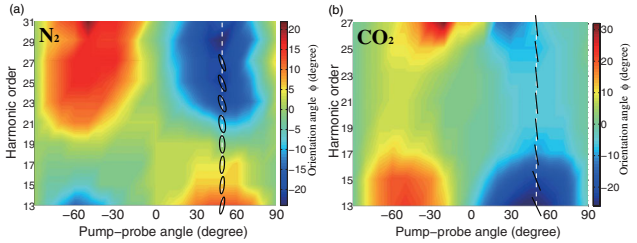

FIG. 3 (color online). Interpolated map of the orientation angle ϕ in degrees for different harmonic orders and molecular orientations for (a) N_2 and (b) CO_2. The HHG ellipse at $\theta = 50°$ for harmonic orders 13–27 is also illustrated. Straight lines represent the harmonic polarization in CO_2 since the ellipticity is small. The uncertainty in this measurement is ±2°.

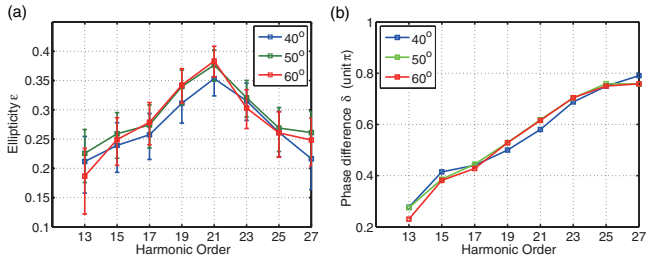

FIG. 4 (color online). (a) Ellipticity ε for relative angles between the pump and probe of $\theta = 40°$, 50°, and 60°, as a function of harmonic order for N_2. (b) Calculated phase difference δ between the parallel and perpendicular components of HHG emission in N_2.

ual driving laser ellipticity will enhance or suppress I_{min}/I_{max} depending on the sign of alignment angle θ, we can confirm the fidelity of the data from the small difference (<0.02 for N_2) in the measured I_{min}/I_{max} for $\pm\theta$ angles. This difference is significantly smaller than the experimentally observed change in I_{min}/I_{max} for most harmonic orders, and is taken into account when determining the error bar of ε shown in Fig. 4(a). The values of ε are averaged for positive and negative θ angles to further reduce errors.

From the measured ellipticity ε and orientation angle ϕ of the N_2 HHG polarization ellipse, we can extract the phase difference δ between the polarization components, using the formulae $\sin(2\chi) = \sin(2\gamma)\sin(\delta)$ and $\tan(2\phi) = \tan(2\gamma)\cos(\delta)$ [20]. The extracted value of δ for $\theta = 40°$, 50°, and 60° degrees for different harmonic orders is plotted in Fig. 4(b) for N_2. The phase difference is almost independent of the molecular orientation angle θ, and gradually increases from 0.2π to 0.8π between harmonic order 13 and 27. For harmonic order 19, the relative phase δ is nearly $\pi/2$. (Since we do not measure the handedness of the beam, there is an ambiguity in the sign of δ.)

As pointed out in [16], for a plane wave recombination dipole, the phase difference between the $\boldsymbol{y}$ and $\boldsymbol{x}$ components of the harmonic emission is either 0 or π. Thus, HHG should be linearly polarized when driven by linearly polarized light. Moreover, the position of any phase jump arising, for example, from a quantum interference effect should depend on the molecular orientation angle. Using a recently demonstrated molecular interferometry technique to measure the phase of the harmonic emission from N_2 during a rotational revival with parallel polarized pump and probe beams, we found that the phase of the harmonic emission from N_2 *does not* depend on orientation of the molecule, and that there is *no* angle-dependent intensity minimum for harmonic orders 19–31. Therefore, the observed significant but smooth variation in phase difference over 8 harmonic orders cannot be fully explained by assuming a plane wave recombination dipole. Our results possibly indicate a breakdown of the plane wave approximation, which could result in a phase delay between the oscillating dipole in the $\boldsymbol{y}$ and $\boldsymbol{x}$ directions. In principle, both the signature of the HOMO on the ionized electron wave packet and the influence of the Coulomb potential on the recolliding electron could generate this phase delay [21]. The contribution from lower-lying molecular orbitals is another potential reason for the observed ellipticity [22]. Thus, the observed HHG ellipticity in N_2 may reflect nontrivial electronic dynamics.

In summary, we found that elliptically polarized harmonics can be emitted by N_2 driven by linearly polarized laser fields, and that the phase difference between the $\boldsymbol{y}$ and $\boldsymbol{x}$ components of the HHG field strongly depends on the harmonic order, but not the molecular orientation. Thus, although N_2 is a simple diatomic and was used for molecular tomography experiments, the strong field approximation and single active electron models cannot completely describe the behavior of harmonic emission from N_2.

The authors gratefully acknowledge support from the DOE and the NSF and useful discussions with Dr. Xinhua Xie, Dr. A. Scrinzi, Dr. Ivan Christov, Dr. O. Smirnova, and Dr. M. Ivanov.

*Xibin.Zhou@colorado.edu

[1] J. Itatani *et al.*, Nature (London) **432**, 867 (2004).
[2] T. Kanai, S. Minemoto, and H. Sakai, Nature (London) **435**, 470 (2005).
[3] N. L. Wagner *et al.*, Proc. Natl. Acad. Sci. U.S.A. **103**, 13279 (2006).
[4] S. Baker *et al.*, Science **312**, 424 (2006).
[5] M. Lein, J. Phys. B **40**, R135 (2007).
[6] S. Ramakrishna and T. Seideman, Phys. Rev. Lett. **99**, 113901 (2007).
[7] X. B. Zhou *et al.*, Phys. Rev. Lett. **100**, 073902 (2008).
[8] K. C. Kulander and B. W. Shore, Phys. Rev. Lett. **62**, 524 (1989).
[9] J. L. Krause, K. J. Schafer, and K. C. Kulander, Phys. Rev. Lett. **68**, 3535 (1992).
[10] P. B. Corkum, Phys. Rev. Lett. **71**, 1994 (1993).
[11] S. Patchkovskii *et al.*, J. Chem. Phys. **126**, 114306 (2007).
[12] O. Smirnova, M. Spanner, and M. Ivanov, Phys. Rev. A **77**, 033407 (2008).
[13] W. Li *et al.*, Science **322**, 1207 (2008).
[14] A. T. Le *et al.*, J. Phys. B **41**, 081002 (2008).
[15] W. Boutu *et al.*, Nature Phys. **4**, 545 (2008).
[16] J. Levesque *et al.*, Phys. Rev. Lett. **99**, 243001 (2007).
[17] V. H. Le *et al.*, Phys. Rev. A **76**, 013414 (2007).
[18] P. Antoine *et al.*, Phys. Rev. A **55**, 1314 (1997).
[19] B. L. Henke, E. M. Gullikson, and J. C. Davis, At. Data Nucl. Data Tables **54**, 181 (1993).
[20] M. Born and E. Wolf, *Principle of Optics* (Cambrige University Press, Cambridge, 1999).
[21] X. H. Xie *et al.*, Phys. Rev. Lett. **101**, 033901 (2008).
[22] O. Smirnova *et al.* (to be published).